RESEARCH   **Open Access**

Bioprospecting CAZymes repertoire of *Aspergillus fumigatus* for eco-friendly value-added transformations of agro-forest biomass

Namrata Joshi[1], Jasneet Grewal[1], Lukasz Drewniak[1] and Kumar Pranaw[1*]

Abstract

Background Valorizing waste residues is crucial to reaching sustainable development goals and shifting from a linear fossil-based economy to a circular economy. Fungal cell factories, due to their versatility and robustness, are instrumental in driving the bio-transformation of waste residues. The present work isolated a potent strain, i.e., *Aspergillus fumigatus* (ZS_AF), from an ancient Złoty Stok gold mine, which showcased distinctive capabilities for efficient hydrolytic enzyme production from lignocellulosic wastes.

Results The present study optimized hydrolytic enzyme production (cellulases, xylanases, and β-glucosidases) from pine sawdust (PSD) via solid-state fermentation using *Aspergillus fumigatus* (ZS_AF). The optimization, using response surface methodology (RSM), produced a twofold increase with maximal yields of 119.41 IU/gds for CMCase, 1232.23 IU/gds for xylanase, 63.19 IU/gds for β-glucosidase, and 31.08 IU/gds for FPase. The secretome profiling validated the pivotal role of carbohydrate-active enzymes (CAZymes) and auxiliary enzymes in biomass valorization. A total of 77% of carbohydrate-active enzymes (CAZymes) were constituted by glycoside hydrolases (66%), carbohydrate esterases (9%), auxiliary activities (3%), and polysaccharide lyases (3%). The saccharification of pretreated wheat straw and PSD generated high reducing sugar yields of 675.36 mg/g and 410.15 mg/g, respectively.

Conclusion These findings highlight the significance of an efficient, synergistic, and cost-effective arsenal of fungal enzymes for lignocellulosic waste valorization and their potential to contribute to waste-to-wealth creation through solid-waste management. The utilization of *Aspergillus fumigatus* (ZS_AF) from an unconventional origin and optimization strategies embodies an innovative approach that holds the potential to propel current waste valorization methods forward, directing the paradigm toward improved efficiency and sustainability.

Keywords Lignocellulosic waste, Pine sawdust, Solid-state fermentation, Response surface methodology, Secretome analysis, Enzymatic hydrolysis

Background

To effectively address the detrimental impacts of fossil fuels, it is widely acknowledged that sustainable development necessitates a shift from the existing linear economic system to a circular model. The primary objective of the circular model is to create a sustainable and regenerative economic system by reducing dependency on finite resources and promoting the use of renewable

*Correspondence:
Kumar Pranaw
k.pranaw@uw.edu.pl; kpranaw@gmail.com
[1] Department of Environmental Microbiology and Biotechnology, Institute of Microbiology, Faculty of Biology, University of Warsaw, Miecznikowa 1, 02-096 Warsaw, Poland

Joshi *et al. Biotechnology for Biofuels and Bioproducts*   (2024) 17:3

Page 2 of 13

biomass feedstocks [1]. With a worldwide annual production of 1×10^{10} metric tons, lignocellulosic biomass has piqued the interest of researchers, accounting for approximately half of the biosphere's total biomass reserves [2]. Due to their abundance, low cost, and sustainable nature, agricultural and forest residues constitute a compelling supply of lignocellulosic biomass feedstock. Lignocellulosic biomass mainly comprises cellulose, hemicellulose, and lignin, with minor amounts of extractives and inorganic components varying according to the wood, grass, or sedge type.

Among the forest residues, sawdust from pine [3], poplar [4], birch [5], eucalyptus [6], etc., cultivated worldwide, represents a major low-cost by-product abundantly available from wood transformation processes but not effectively utilized due to their structural heterogeneity and recalcitrance [7]. According to the European Organization of Sawmill Industries (EOS), sawdust production averaged 13.4 million m³ between 2020 and 2022. Depending on market demand, sawdust can be supplied to the particle board industry, utilized as a renewable fuel to produce bio-energy (e.g., pellets manufacture), or subjected to various procedures for the valorization of its cellulose, hemicellulose, and lignin fractions [8, 9]. However, in practice, the substantial sawdust volumes are improperly disposed of, posing significant environmental risks to air, water, and soil quality. Burning leftover sawdust outdoors pollutes the air and has unfavorable consequences for the land, such as raising its acidity levels [10]. Thus, implementing measures to properly manage leftover sawdust can alleviate environmental problems connected with its mishandling and provide economic benefits [11].

In this context, deploying sawdust as a solid substrate for cultivating microorganisms via solid-state fermentation (SSF) can be a simple, low-investment approach for producing value-added products like hydrolytic enzymes with varied biorefinery applications. SSF has advantages over submerged fermentation (SmF), including lower operational expenses, little chance of contamination, easy enzyme recovery, and the production of enzymes with higher efficiency, specific activity and easy recovery [12, 13]. However, unlike conventional agro-residues such as wheat, rice straw, corn stover, and sugarcane bagasse used as attractive fermentable materials, the reports on the usage of sawdust as a supporting matrix for biotransformation are scanty. Furthermore, the nutritional profile of pine sawdust (PSD) due to the presence of lignin-derived phenolic, resinous compounds makes it less favorable for the growth of microbes [14]. Nevertheless, fungi, with their well-known adaptability and resilience to harsh environmental conditions and a diverse arsenal of extracellular enzymes, can play a critical role in depolymerizing these complex, underutilized substrates into various valuable metabolites through SSF.

The goal of the current study was to isolate lignocellulolytic fungi from the wooden remnant structures, the scaffolding of the mine's tunnels and corridors, taking into account that extreme environmental niches like the abandoned Złoty Stok gold mine (southwestern Poland) can be a vital source of robust adaptive organisms [15, 16]. The isolated fungi were evaluated for their biotransformation potential by pine sawdust (PSD) valorization to produce economic hydrolytic enzymes (cellulases, xylanases and β-glucosidases). To further gain insight into the lignocellulose deconstruction potential of the selected isolate, i.e., *Aspergillus fumigatus* (ZS_AF), statistical optimization of SSF critical process parameters and secretome analysis was conducted using LC–MS/MS. The CAZymes (carbohydrate-active enzymes) repertoire of *A. fumigatus* grown on PSD is scanty. Although the secretome profile varies with environmental circumstances, the discoveries will open up new avenues for waste management regarding economic value generation. Lastly, cheaply produced hydrolytic enzymes used wheat straw (WS) and PSD as model substrates for saccharification. The released fermentable sugars can generate a plethora of high-value acids, materials, platform chemicals, etc., to meet commercial demands, while the residual solid substrates can be added back to the soil to act as a carbon sink.

Results and discussion

Molecular identification of the isolated cellulolytic fungus

On the 5th day of incubation, *A. fumigatus* from an ancient gold mine with the highest cellulolytic activity, i.e., CMCase and FPase with 6.33 and 1.0 IU/ml, respectively, was chosen for further study. The fungus was identified based on differences in the ITS region sequencing. BLAST analysis was used to determine the similarity of the ZS_AF sequence to that of *Aspergillus fumigatus*, and evolutionary analysis was performed using the MEGA 11 program (as shown in Additional file 1: Fig. S1a). Furthermore, the sequence of *A. fumigatus* was submitted to the NCBI GenBank database under the accession number OM258166.

Statistical optimization of hydrolytic enzyme production

The employment of a regression model, particularly the response surface methodology (RSM), facilitated the exploration and maximization of enzyme production from the fungus *Aspergillus fumigatus* (ZS_AF). Based on the constant one variable at a time (COVT) approach, the enzyme yields of 60.7 IU/gds CMCase, 668.14 IU/gds xylanase, 56.4 IU/gds β-glucosidase, and 11.2 IU/gds FPase were obtained in SSF under

optimized conditions of 5 g PSD as a substrate, 5 days of incubation, pH 7.0, and temperature 30 ℃. For instance, Matrawy et al. [17], demonstrated a similar approach, employing RSM to optimize enzyme production. This work illustrated the practical application and validity of the regression model in enhancing enzyme yields, aligning with the methodology employed in our study. The SEM images supported the luxuriant proliferation of *A. fumigatus* over PSD during SSF (Additional file 1: Fig. S1b, c). For the maximal yields of all four enzymatic activities and the interactive effects of physical factors such as production media pH, temperature, and incubation time on enzyme production, RSM was employed using a rotatable central composite design (RCCD). Moreover, a statistical model for the effects of these factors was derived from the RCCD experiments, where the observed and predicted responses for CMCase, xylanase, β-glucosidase, and FPase were in good agreement (Table 1). Three-dimensional response surface plots (Fig. 1) were created using the models to show the individual and interacting effects of the process factors. The ANOVA results of the quadratic response-surface model fitting for CMCase, xylanase, β-glucosidase, and FPase are presented in Additional file 1: Tables S1, S2, S3, and S4, respectively. The analysis of variance revealed that selected parameters (i.e., pH, temperature, and time) were highly significant in the production of hydrolytic enzymes. The F-value compares the lack of fit variance to pure error variance. A significant model has a high F-value. Thus, the attained respective values for CMCase (11390.12), xylanase (2082.73), β-glucosidase (52.29), and FPase (47.27) indicated that the model was significant for the production of all four enzymatic activities.

The Fisher F test also indicated significance, with a probability value well below the threshold ($P >$ F—0.0001). There was little probability that noise could have produced a "Model *F*-value" this significant (0.01%), which means the model could explain 99.99% of the total variation, including the sample variation, but not the final 0.01%. Model terms with "Prob > *F*" values less than 0.0500 were considered significant. The signal-to-noise ratio is measured by "Adequate Precision". It contrasts the average prediction error with the range of the anticipated values at the design points. A ratio of at least 4 is preferred, and the signal-to-noise ratios for CMCase, xylanase, β-glucosidase and FPase in the current investigation were 392.084, 166.179, 29.068, and 27.653, respectively, indicating a sufficient signal. The regression equation generated a coefficient of determination (R^2) of 0.9999 for CMCase, 0.9995 for xylanase, 0.9792 for β-glucosidase, and 0.9770 for FPase. The findings indicated that the quadratic model was remarkably

significant and could account for nearly 95% of the variance in enzyme production.

Additionally, Additional file 1: Fig. S2 shows normal probability plots (i.e., a-d) for enzyme production of CMCase, xylanase, β-glucosidase, and FPase, respectively. The normal probability plot of residuals is a crucial diagnostic tool for identifying and clarifying any systematic deviations from the assumptions that errors are independently distributed with normal distribution and that the variances of errors are homogeneous. The average (percentage) probability plot of "Studentized" residuals suggests hardly any breach in the assumptions underlying the analyses.

After RCCD analysis, the optimal physical conditions for all three factors were determined to be pH 7.0, temperature 40 ℃, and incubation period of 5 days. The model anticipated that under the aforementioned optimum conditions, the enzyme yield for CMCase, xylanase, β-glucosidase, and FPase would reach a maximum of 126.34 IU/gds, 1429.53 IU/gds, 68.82 IU/gds, and 34.47 IU/gds, respectively. Consequently, in validation experiments conducted at the optimized values of the test variables specified by the model, the maximum enzyme production for CMCase, xylanase, β-glucosidase, and FPase was measured to be 119.41 IU/gds, 1232.23 IU/gds, 63.19 IU/gds, and 31.08 IU/gds, respectively. These outcomes were consistent with the predictions of the model. Hereafter, successful optimization using RSM resulted in an approximately twofold increase in the production of hydrolytic enzymes from the initial amount. In another study, Azzouz et al. [18] demonstrated significant enhancements through the OFAT and RSM methods, achieving maximum values of 4008.25 ± 3.73 U/gds and 5427.51 ± 4.4 U/gds, respectively. These values were notably higher than the initial conditions, which yielded 1899.02 ± 1.6 U/gds. Similarly, Kumar et al. [19] resulted in a 3.35-fold improvement in FPase activities after optimizing the medium components and concentrations using the RSM approach as compared with the un-optimized conditions un-optimized conditions. To the best of the authors' knowledge, the titres of hydrolytic enzymes obtained using PSD as a substrate are the highest ones reported to date. Furthermore, these yields are also equivalent to those reported from other popular and conventional agro-forest biomass, as listed in Table 2. These findings offer novel opportunities to valorize an underutilized but readily available waste resource.

Secretome analysis of degradative proteins released by *A. fumigatus* cultured on PSD

To complement the obtained enzymatic titres and elucidate the holistic enzymatic repertoire employed during solid substrate degradation, secretome analysis using

Table 1 RCCD experimental design developed using Design-Expert version 7.0.0 software

Run no.	Factor A pH	Factor B temperature	Factor C time	Different responses								
				CMCase (IU/gds)		Xylanase (IU/gds)		β-Glucosidase (IU/gds)		FPase (IU/gds)	
				Observed	Predicted	Observed	Predicted	Observed	Predicted	Observed	Predicted
1	7	20	5	42.92	42.50	681.76	688.47	47.48	22.99	23.74	22.99
2	11	20	5	50.08	50.11	651.35	658.15	41.70	20.22	20.85	20.22
3	7	40	5	126.31	126.34	1434.66	1429.54	69.35	34.47	34.68	34.47
4	11	40	5	121.90	121.75	548.64	555.37	74.34	36.06	37.19	36.06
5	7	20	9	80.40	80.43	853.34	847.35	54.87	27.45	27.43	27.45
6	11	20	9	82.26	82.11	749.18	755.04	53.95	26.35	27.25	26.35
7	7	40	9	118.76	118.60	1315.1	1309.05	61.37	30.06	30.54	30.06
8	11	40	9	107.77	108.06	378.86	372.89	67.97	33.30	33.66	33.30
9	5.64	30	7	91.15	91.40	1361.96	1368.54	61.54	30.95	30.64	30.95
10	12.36	30	7	89.01	88.94	563.46	555.83	60.28	31.35	30.09	31.35
11	9	13.18	7	44.56	44.81	419.06	411.47	31.57	16.61	15.79	16.61
12	9	46.82	7	137.21	137.14	706.74	713.28	62.93	32.11	31.34	32.11
13	9	30	3.64	81.91	82.14	976.24	967.61	57.77	29.97	28.89	29.97
14	9	30	10.36	102.60	102.54	940.19	947.77	61.83	31.41	30.92	31.41
15	9	30	7	89.90	89.95	833.21	834.59	54.77	26.62	27.39	26.62
16	9	30	7	89.90	89.95	846.26	834.59	55.00	26.62	27.50	26.62
17	9	30	7	90.34	89.95	831.34	834.59	53.23	26.62	26.61	26.62
18	9	30	7	90.36	89.95	832.59	834.59	52.77	26.62	26.38	26.62
19	9	30	7	89.77	89.95	833.21	834.59	52.14	26.62	26.07	26.62
20	9	30	7	89.44	89.95	830.72	834.59	52.96	26.62	26.01	26.62

X1 = A: pH   Actual Factor
X2 = B: Temp   C: Time = 7.00
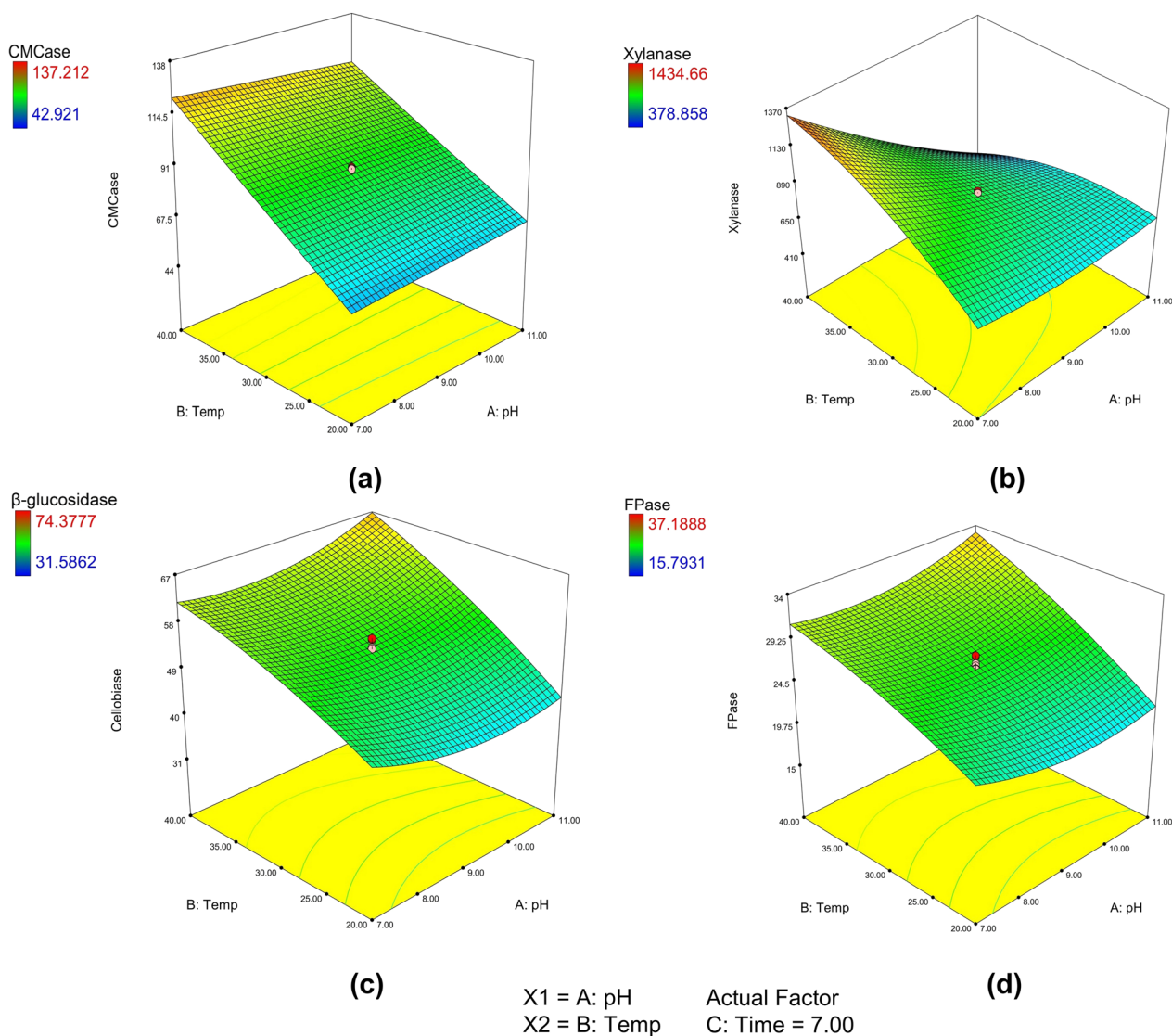
Fig. 1 The response surface contour plot and 3D response plot for *A. fumigatus* enzymes **a** CMCase, **b** xylanase, **c** β-glucosidase, and **d** FPase as a function of pH (**A**), temperature (**B**), and time (**C**)

Table 2 Comparative analysis of cellulolytic and xylanolytic enzymes produced by *Aspergillus* sp. growing on different agro-forest waste

Substrate	CMCase activity (IU/gds)	Xylanase activity (IU/gds)	β-Glucosidase activity (IU/gds)	FPase activity (IU/gds)	Reference
Rice straw	235	180	190	12.5	[48]
Brewery spent grain	3.24	2279.9	–	–	[49]
Biomass sorghum	41.47	300.07	63.61	–	[50]
Sugarcane bagasse	4.20	–	–	0.64	[51]
Wheat bran	20.5	–	87.6	7.8	[52]
Pine sawdust	119.41	1232.23	63.19	31.08	Present study

LC–MS/MS was conducted. This integrated approach not only identifies key CAZymes but also sheds light on their coordinated action, enhancing valorization prospects by *A. fumigatus*. By employing PSD as a substrate, extracellular protein secretion from *A. fumigatus* during SSF was carried out. The study found 69 proteins, 77% of which were carbohydrate-active enzymes (CAZymes) (http://www.cazy.org), with 62% glycoside hydrolases (GH), 9% carbohydrate esterases (CE), 3% auxiliary activities (AA), and 3% polysaccharide lyases (PSL) (as illustrated in Fig. 2). The remaining 23% comprised hypothetical proteins, oxidoreductase, lipase, and chitinase. The study also revealed that the molecular weights of the identified proteins ranged from 12.9 to 117.2 kDa, with most of the proteins being acidic, as indicated by their isoelectric points (pI) ranging from 4 to 7. This finding was consistent with previous studies by [20, 21], who reported similar molecular weight and pI observations. As glycoside hydrolases (GH) break down lignocellulosic biomass, endoglucanases (EGs) primarily act on the amorphous region of glycosidic linkages through hydrolysis. Cellobiohydrolases (CBHs) release cellobiase by acting on the reducing and non-reducing ends of chains, while β-glucosidases liberate glucose as the end product [22]. The secretome analysis conducted in this study revealed that among all GH families, GH5 (10%), GH12 (3%), and GH16 (3%) were the most abundant, dominated by endoglucanases, followed by GH7 (6%) and GH6 (3%) which included cellobiohydrolases. In addition to cellulose-degrading enzymes, endoxylanases and xylosidases from families such as GH11 (3%), GH43 (3%), and GH10 (1%) were also observed. Adav et al. [23] observed a comparable dominance of endoglucanases and cellobiohydrolases from the GH5 and GH7 families in the *A. fumigatus* secretome. The remaining CAZymes families are involved in the degradation of other polysaccharides, such as pectin, classified under GH28, CE8, CE12, and PL1 families. The study also detected the presence of the AA9 family, including lytic polysaccharide monooxygenases (LPMOs), and various carbohydrate-binding module (CBM) families, such as CBM1 (primarily found in fungi), CBM20, CBM42, CBM19, and CBM43. The finding of secretome emphasizes the range of CAZymes produced by *A. fumigatus* during solid-state fermentation of PSD and the ability of *Aspergillus* to valorize non-conventional recalcitrant substrate.

Structural analysis and enhancement of hydrolysis efficiency by *Aspergillus*-derived enzyme

The morphological structure of both substrates, i.e., PSD and WS, were examined by SEM (Fig. 3). The surface of raw PSD and WS (Fig. 3a, d) exhibited stiff, meticulously ordered fibrils, whereas, after pretreatment, their structure tends to be less ordered and leads to the formation of pores or gaps (a red arrow in Fig. 3b, e) facilitating increased availability of cellulose surface area for enzyme attack. Similarly, further disrupted fibers showed more fractures after hydrolysis (blue arrow in Fig. 3c, f).

Fig. 2 Compositional study of total proteins found in the secretome of *A. fumigatus* identified during SSF with PSD. Percentage (%) of differentially expressed CAZymes include glycoside hydrolases (GH), auxiliary activities-related enzymes (AA), carbohydrate esterases (CE), polysaccharide lyases (PL), and other non-CAZymes
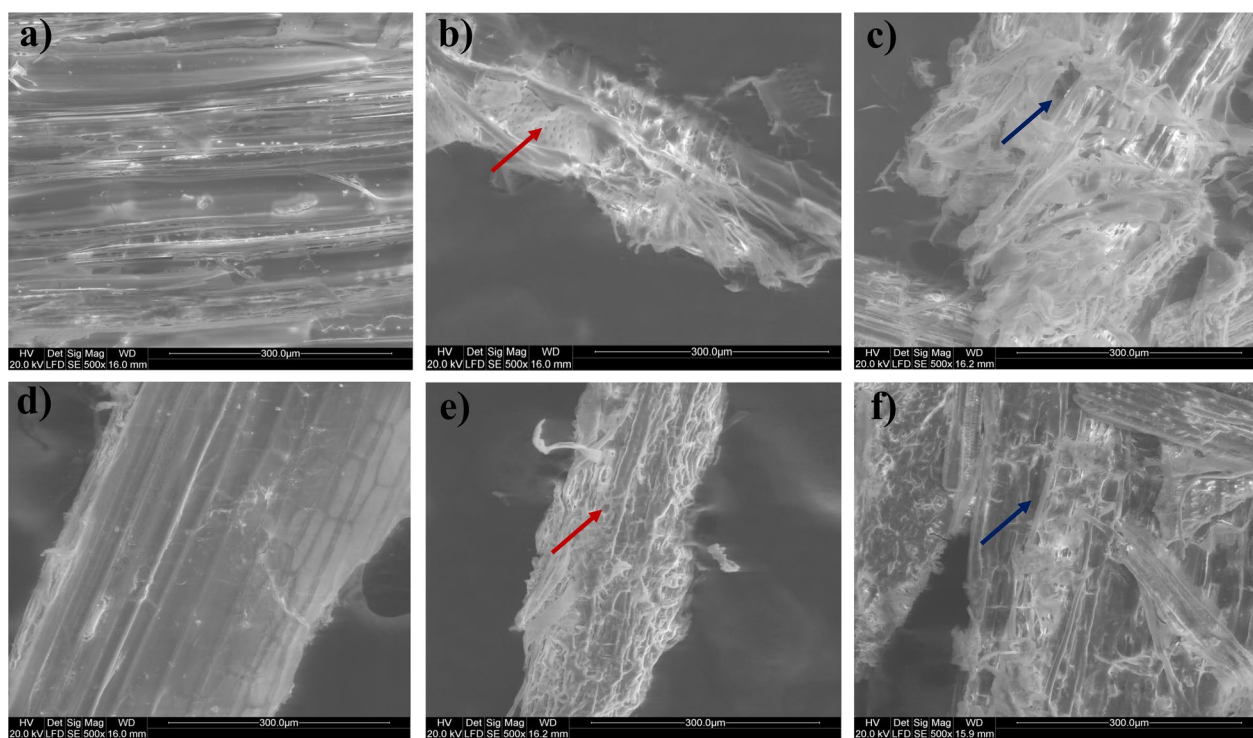
Fig. 3 SEM detection of pine sawdust **a** untreated; **b** alkali-pretreated; **c** hydrolyzed with *A. fumigatus*-derived enzyme and wheat straw **d** untreated; **e** alkali-pretreated; **f** hydrolyzed wheat straw

Likewise, structural disruption has also been observed in many studies with various pretreatment techniques [24, 25]. The effect of alkali pretreatment in both substrates was further supported by FTIR spectra, which showed a diminution in the absorption peak at 3437 cm^{-1} as a result of the stretching of the O-H bond of the phenol group of cellulose and lignin in comparison to the untreated substrate (Additional file 1: Fig. S3a, b). Similarly, alkaline pretreatment resulted in a disturbance in another peak at 1742 cm^{-1}, representing the disruption of C=O stretching in the acetyl ester and carbonyl aldehyde units of hemicellulose and lignin, indicating the successful breakdown of hemicellulose and lignin from both substrates. Another shift in the peak at 1375 cm^{-1}, corresponding to C-H deformation in cellulose and hemicellulose, was noticed, resulting in a declining trend and the peak at 1236 cm^{-1}, complementary to disruption of C-O stretching in lignin fraction following processing [26, 27].

Furthermore, XRD was utilized to analyze the crystallinity of both PSD and WS raw substrates and treated with a pretreatment approach and subsequent hydrolysis, as shown in Additional file 1: Fig. S4a, b. The XRD pattern showed distinctive peaks at 2 values of 18.5° and 22.5°, corresponding to the (101) and (002) lattice planes of crystalline cellulose type I, respectively [28]. The alkali-pretreated PSD and WS showed a considerable rise in crystallinity index (CrI) of 73.21% and 68.9% compared to the untreated PSD and WS, which had a CrI of 44.2 and 58%, respectively. This rise in CrI was attributable to the pretreatment method, which increased the cellulose content by removing lignin and hemicellulose. A similar increase in CrI after pretreatment was also observed in earlier studies [4, 25]. Furthermore, after the alkaline pretreatment procedures, 4% decrease in CrI following hydrolysis in both substrates was observed due to more extensive structural disruption.

Following the PSD and WS structural analysis, the enzymatic hydrolysis was investigated using an *A. fumigatus*-derived enzyme during SSF with PSD. After 72 h of hydrolysis, alkaline pretreated WS with 30 FPU/g cellulase loading yielded 675.26 mg/g reducing sugar. Likewise, using PSD as a substrate for saccharification resulted in a sugar yield of 410.15 mg/g using 150 FPU/g of cellulase loading (Fig. 4). As compared to untreated substrates, the hydrolysis yield of alkaline pretreated PSD and WS was enhanced by 50.15% and 75.5%, respectively. Due to the higher crystalline nature of PSD compared to WS, a higher cellulase loading was required. Liang et al. [4] and Kruyeniski et al. [29] discovered a ~55% and ~25% hydrolysis yield for two types of sawdust, popular and pine sawdust. Similarly, Jin et al. [7] found that pine and catalpa sawdust yielded 44.59 and 39.76 mg/g of reducing
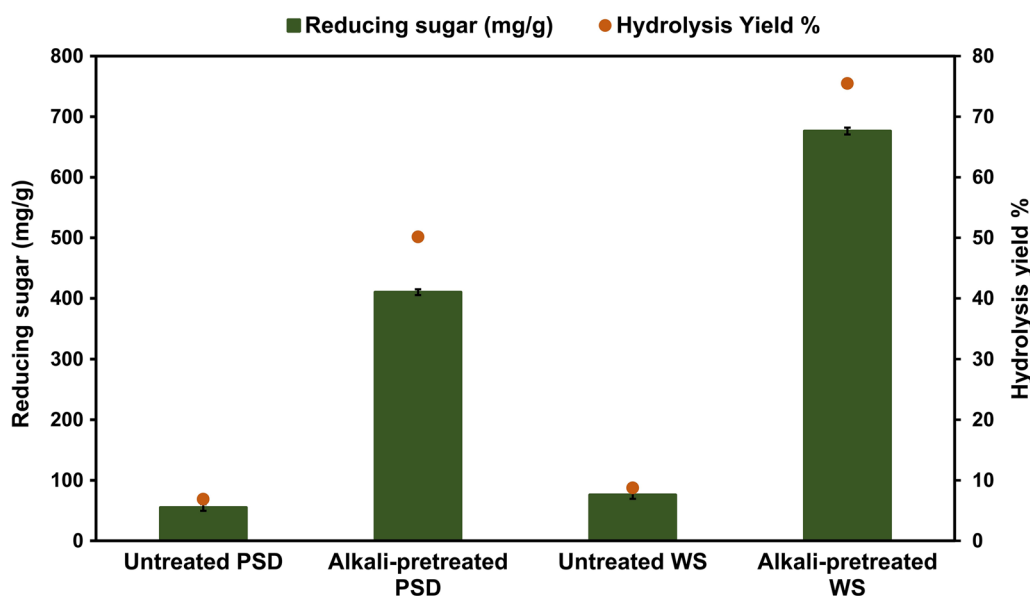
Fig. 4 Saccharification potential of *A. fumigatus* on untreated and alkali-pretreated WS and PSD

sugar yield, respectively. Notably, utilizing pine sawdust with its endogenously produced enzymes led to a higher reducing sugar yield while avoiding costly purification procedures. In contrast to earlier investigations, Table 3 shows that utilization of WS during saccharification resulted in significantly more reducing sugar than other reports. Zabihi et al. [30] and Ilanidis et al. [31] achieved 480 kg/ton and 336.41 g/kg of reducing sugar using commercial cellulase (ASA Spezialenzyme GmbH, Germany and Cellic CTec2) of 15 FPU and 100 CMCase, respectively. Additionally, reducing sugar generation using hydrolyze derived from fungi such as fungus consortium

release reducing sugar of 402.38 mg/g [32]; *Sporotrichum thermophile* 281 mg/g [33]; *Phoma exigua* 177.2 mg/g [34] of wheat straw. The outcomes of this study were also compared to those of other lignocellulosic biomass sources. Catalpa sawdust produced 136.44 mg/g of reducing sugar [35], whereas raw wheat straw and rice straw yielded 130.24 mg/g and 125.36 mg/g of reducing sugar, respectively [36]. Using grass clippings as a substrate, on the other hand, provided a significantly more significant amount of reducing sugar at 229.42 mg/g [7]. It addresses the problems associated with waste management and the negative impacts that waste burning and

Table 3 Yield of reducing sugars obtained from enzymatic hydrolysis of pretreated wheat straw

Pretreatment method	Source of enzyme used for saccharification	Temperature (°C)	Enzyme loading (per g of wheat straw)	Reducing sugars (mg/*g* wheat straw)	Reference
Acetic acid/steam explosion/supercritical carbon dioxide pretreatment	Commercial cellulase (ASA Spezialenzyme GmbH, Germany)	50	15 FPU	336.41	[30]
Hydrothermal pretreatment	Cellic CTec2 (Sigma-Aldrich, Germany)	50	100 CMCase	480.00	[31]
Ammonium sulfite pretreatment with sodium carbonate supplementation	Commercial cellulase and xylanase (Imperial Jade Bio-Technology Co., Ltd. Yinchuan, China)	50	35 FPU cellulase and 70 FXU xylanase	413.00	[53]
[EMIM][Ac] Ionic liquid pretreatment	*Sporotrichum thermophile* xylanase	40	160 U	281.00	[33]
Acid pretreatment	*T. reesei* NCIM 1186	50	30.85 CMCase	371.44	[54]
Alkali pretreatment	*Phoma exigua* secretome	55	15.23 FPU	101.16	[34]
Acid pretreatment	*Penicillium janthinellum* EMS-UV-8 cellulase	50	20 FPU	376.00	[55]
Alkali pretreatment	*Aspergillus fumigatus*	50	30 FPU	675.36	Present study

Joshi *et al. Biotechnology for Biofuels and Bioproducts* (2024) 17:3

Page 9 of 13

accumulation cause on the environment. Addressing these difficulties could improve the economic feasibility of biorefinery processes.

Conclusions

The present study evaluated the use of an unconventional but abundant and recalcitrant lignocellulosic agro-forest residue, i.e., pine sawdust (PSD), for the production of the hydrolytic enzymes using *A. fumigatus*, isolated from an ancient Złoty Stok gold mine. The findings demonstrated that *A. fumigatus* has a significant potential for producing high titers of cellulases and hemicellulases at low cost under SSF. The statistical model optimization (RSM) endorsed that enzyme production primarily affected by physical characteristics like pH, temperature, and time, whose optimal selection increased the yield twofold. The secretome profiling supported the lignocellulosic biomass valorization potential due to the repertoire of diverse CAZymes. Lastly, the high reducing sugar yields obtained from saccharification of pretreated agro-forest residues indicated the potential of this low-cost bioprocess for valorizing waste streams with concomitant generation of high-value commercial commodities with diverse applications.

Materials and methods

Isolation, screening, and identification of potential lignocellulolytic fungus

The samples were collected from an ancient gold mine (Złoty Stok) in southwest Poland (area descriptions and parameters) mentioned by [16]. All samples were transferred to the laboratory in sterile falcons and plastic bags and stored at 4 ℃. To evaluate their cellulolytic potential, a substrate-specific enrichment approach was used. For the isolation process, diluted samples were mixed with Reese's minimal medium (RMM) with the following composition (g/L): 0.5 Peptone (Protease) (CAS number: 91079-38-8); 2.0 KH_2PO4; 0.3 $MgSO_4$; 0.3 KNO_3; 1.4 $(NH_4)_2SO_4$; 0.3 $CaCl_2$; including micronutrients (mg/L), i.e., 5 mg $FeSO_4$; 1.4 mg $ZnSO_4$; 2 mg $CoCl_2$; 5 mg $MnSO_4$, pH 6.0 supplemented with 1% carboxymethyl cellulose (CMC). The inoculated flask with samples was incubated at 25 ℃ for 7 days. Following enrichment, isolates were grown on RMM with 1% CMC (*w/v*) as a substrate using the spread plate technique and producing isolates were selected based on plate assay [37], purified, and maintained on potato dextrose agar (PDA) plates. The fungal cultures were stored at 4 ℃ and subcultured at monthly intervals. The screened sample identified by rDNA sequences was amplified using universal primer pairs, pITS-1 (5-TCC GTAGGTGAACCTGCGG-3) and pITS-4 (5-TCCTCC GCTTATTGATATGC-3). The DNA from the amplified

fragments was sequenced at Eurofins Polska (https://www.eurofins.pl/), and the sequenced amplified product was then BLAST searched at the NCBI database. The MEGA 11 (molecular evolutionary genetics analysis) tool created a phylogenetic tree using the neighbor-joining method to estimate evolutionary distances [38]. Based on quantitative and qualitative screening for higher cellulolytic activity among all isolated fungus strains (data not shown), *Aspergillus fumigatus* ZS_AF (NCBI accession number OM258166) was chosen for further study.

Biomass feedstock and chemicals

PSD and WS were sourced locally from the Poland countryside, partially chopped, and sieved with 20–40 mesh size. Both substrates were dried and stored at room temperature (~22 ℃) for future studies. The chemical composition of both untreated PSD and WS (% *w/w*) were determined by standard NREL procedures as 44.8 ± 0.2; 32 ± 0.25 cellulose, 27.9 ± 0.4; 45.9 ± 0.3 hemicelluloses, and 23.9 ± 0.4; 14.2 ± 0.5 lignin, respectively [39]. All analytical grade chemicals are purchased from Sigma Aldrich (St. Louis, MO, USA).

Solid-state fermentation for hydrolytic enzyme production utilizing PSD as substrate

Five grams of coarsely crushed and sieved (1 mm mesh size) PSD with a substrate-to-moisture ratio of 1:3 utilizing RMM were employed in 200 ml Erlenmeyer flasks for the SSF procedure. *A. fumigatus* spores were grown on PDA for inoculum development. The spores were harvested in sterile Tween-80 (0.1% *v/v*) as it makes the dispersion on water easier, yielding a more consistent procedure for inoculum preparation. Subsequently, each flask was inoculated with a concentration of $\sim 1 \times 10^8$/ ml spores and incubated under static conditions at 30 ℃ for 5 days. The extraction procedure included using a 0.05 M citrate buffer pH 6.0, followed by 1 h of constant shaking at 150 rpm at 30 ℃. The resulting crude extract was subsequently passed through two layers of muslin cloth to remove any remaining solids, and it was then centrifuged at 10,000 rpm for 20 min at 4 ℃. The clear supernatant obtained after centrifugation was stored at 4 ℃ and used for additional investigations of the activities of several hydrolytic enzymes.

Statistical approach for optimizing hydrolytic enzyme production

In the present study, the effect of physical factors such as media pH range (5.0–11.0), temperature (15–40 ℃), and time (3–9 days) on enzyme production was carried out by

the COVT approach. The output of *A. fumigatus* enzymes was significantly affected by these parameters. To further boost the enzyme production, these three parameters were optimized using RSM, including rotatable central composite design (RCCD) using Design-Expert version 7.0.0 software (Stat-Ease Corporation, USA). This software generated 24-factorial design at five levels ($-\alpha$, -1, 0, $+1$, $+\alpha$). Table 1 displays the design matrix comprising 20 experimental runs. The matrix has six axial points, six center points, and eight random factorial points. The response for the designed model was collected from several enzyme activities (i.e., CMCase, xylanase, β-glucosidases, and FPase). The RSM experiments' data were evaluated using analysis of variance (ANOVA). This enabled the study of regression coefficients, prediction equations, and case statistics. The experimental outcomes of RSM were fitted with a second-order polynomial equation (Eq. 1) to enable the estimation of the response variable using independent variables:

$$Y = \beta_0 + \sum_{j=1}^{k} \beta_j X_j + \sum_{j=1}^{k} \beta_{jj} X_j^2 + \sum_i \sum_{<j=2}^{k} \beta_{ij} X_i X_j + e_i. \tag{1}$$

Y represents the response variable in the equation. The intercept coefficient for the model is β_0. The interaction between the linear, quadratic, and second-order terms are denoted by the coefficients β_j, β_{jj}, *and* β_{ij}, respectively. The independent variables are represented by X_i and X_j, where *i* and *j* are values ranging from 1 to k. This study had three independent parameters ($k = 3$). The error is represented by e_i. The statistical model was verified to reflect all variables in the design space accurately. To illustrate how significant variables affected the response, three-dimensional graphics were created.

Assays for determining enzymatic activities

The crude enzyme produced from *A. fumigatus* utilizing PSD during the SSF process was tested for endoglucanase (CMCase), xylanase, β-glucosidase (cellobiase), and filter paper activity (FPase). The endoglucanase activity was examined by dissolving 2% CMC (*w/v*) in 0.05 M citrate buffer pH 6.0 and incubating at 50 ℃ for 30 min. The dinitrosalicylic acid (DNS) method determined the total reducing sugars by UV–visible spectrophotometer at 540 nm. For exoglucanase activity, 50 mg Whatman Filter paper No. 1 was mixed in 0.05 M citrate buffer (pH 6.0) and incubated at 50 ℃ for 60 min to determine the reducing sugar using the Ghose [40] standard method. Similarly, 1% beechwood xylan was employed to test xylanase activity by diluting in 0.05 M citrate buffer pH 6.0 and incubating at 50 ℃ for 30 min. One unit (U) of xylanase activity is the amount of enzyme that releases

1 μmol of xylose per minute. The activity of β-glucosidase was evaluated using p-nitrophenyl-α-D-glucopyranoside as a substrate, and the reaction was stopped by adding glycine buffer (pH 10.8) after incubation. The total amount of p-nitrophenol was determined by measuring absorbance at 405 nm. [41].

Secretome analysis and protein identification by LC–MS/MS

A. fumigatus enzyme extracted in supernatant form during the SSF process was further used for secretome analysis. The proteins were precipitated overnight in ice-cold acetone (80%), and their concentrations were determined using the Bradford method [42]. The mixture was centrifuged for 15 min, and the resultant air-dried pellet was resuspended in 0.2 M ammonium bicarbonate. The protein (20 μg) was subsequently loaded onto 12% SDS-PAGE gel, and the bands were visualized using Coomassie brilliant blue G-250. The gel is chopped into smaller pieces after being sliced into three or four sections. The diced gel was rinsed and destained with 75% acetonitrile (ACN) solution and 25 mM triethylammonium bicarbonate buffer (TEAB). Furthermore, the reduction and alkylation reactions were carried out with 10 mM dithiothreitol and 50 mM iodoacetamide, respectively. The gel pieces were washed twice with TEAB and dehydrated using 100% ACN to remove access to reducing and alkylating agents. The fragmented gel was processed overnight with trypsin at 37 ℃; the resultant tryptic digest was extracted with 5% acetonitrile and 0.1% formic acid before being subjected to LC–MS/MS analysis [21, 23]. Protein identification was carried out using Mascot 2.4.01, and the resulting protein entry was systematically matched against the UniProt database for *A. fumigatus* [43]. The identified proteins were categorized into different glycoside hydrolases (GH) families based on the dbCAN2 tool [44].

Pretreatment and structural analysis of agro-forest residues subjected to saccharification by produced hydrolytic enzymes

Following Jin et al. [35] with some adjustments, both PSD and WS were treated with 5% (*w/v*) alkali (NaOH) solution. The suspension was kept in an oil bath at 120 ℃ for 30 min. After cooling, the pretreated solids were meticulously washed with distilled water until they attained a neutral pH. The solid leftovers were collected and dried overnight. Similarly, the structural change on raw, alkali-pretreated, hydrolyzed PSD and WS was conducted using scanning electron microscopy (SEM). Fourier transform infrared spectroscopy (FTIR) for observing changes in the functional groups and X-ray diffraction (XRD) to elucidate the cellulose crystallinity by determining the crystallinity index (CrI) was calculated using Eq. 2 [45]:

$$\text{Crystallinity index (CrI)} = \frac{\text{Crystalline portion (I}_{002}) - \text{amorphous portion (I}_{AM})}{\text{Crystalline portion}} \times 100\%, \tag{2}$$

where (I_{002} = intensity at $2\theta = 22.5$ and I_{AM} = intensity at $2\theta = 18.5$).

Enzymatic hydrolysis of lignocellulosic substrates

The enzyme attained from the SSF process under optimum conditions was utilized to hydrolyze both substrates, i.e., PSD and WS. Specifically, 150 FPU/gds of PSD and 30 FPU/gds of WS containing 0.005% (w/v) sodium azide were used to saccharify the substrates at 50 ℃ under 150 rpm for durations of 24, 48, and 72 h. Untreated PSD and WS were used as controls, with the same enzyme concentrations as the treated samples. After centrifugation, the clear supernatant was collected at various time intervals (24, 48, and 72 h), and the reducing sugars were measured using the DNS method [46]. Each condition was tested in triplicate. The hydrolysis yield was determined using Eq. 3 [47]:

$$\text{Yield of hydrolysis (\%)} \frac{\text{Reducing sugar (g) x 0.9}}{\text{Polysaccharide in a substrate (g)}} \times 100. \tag{3}$$

Statistical analysis

RSM was used to investigate the optimization data subjected to analysis of variance (ANOVA) in a rotatable central composite design (RCCD). The experiment values shown in graphs and tables are the mean±SD of three replicates determined in MS Excel.

Abbreviations

PSD	Pine sawdust
RSM	Response surface methodology
CAZymes	Carbohydrate-active enzymes
SSF	Solid-state fermentation
CMC	Carboxymethyl cellulose
RMM	Reese's minimal medium
WS	Wheat straw
PDA	Potato dextrose agar
RCCD	Rotatable central composite design
ANOVA	Analysis of variance
DNS	Dinitrosalicylic acid
ACN	Acetonitrile
TEAB	Triethylammonium bicarbonate buffer
GH	Glycoside hydrolases
CE	Carbohydrate esterases
CBM	Carbohydrate-binding module
COVT	Constant one variable at a time
SEM	Scanning electron microscopy
XRD	X-ray diffraction
CrI	Crystallinity index
FTIR	Fourier transform infrared spectroscopy
FPase	Filter paper activity
NREL	National renewable energy laboratory

Supplementary Information

The online version contains supplementary material available at https://doi.org/10.1186/s13068-023-02453-6.

Additional file 1: Fig. S1 a A phylogenetic tree for *A. fumigatus* based on ITS sequence, **b** *A. fumigatus* spores grown over PDA plates; magnification captured at 4000× **c** *A. fumigatus* growth over PSD, magnification captured at 4000×. **Fig. S2** Residual diagnostics of contour surface of the quadratic model by Normal plot of residuals for **a** CMCase, **b** xylanase, **c** β-glucosidase and **d** FPase production. **Fig. S3** FTIR spectra of untreated, alkali-pretreated, and hydrolyzed **a** Pine sawdust (PSD) and; **b** Wheat straw (WS). **Fig. S4** XRD diffraction of untreated, alkali-pretreated and hydrolyzed **a** Pine sawdust (PSD) and **b** Wheat straw (WS). **Table S1** Regression analysis for the production of CMCase enzyme by *A. fumigatus* under SSF for quadratic response surface model fitting ANOVA. Where X1= pH, X2= Temperature and X3= Time. **Table S2** Regression analysis for the production of xylanase enzyme by *A. fumigatus* under SSF for quadratic response surface model fitting ANOVA. Where X1= pH, X2= Temperature and X3= Time. **Table S3** Regression analysis for the production of β-glucosidase enzyme by *A. fumigatus* under SSF for quadratic response surface model fitting ANOVA. Where X1= pH, X2= Temperature and X3= Time. **Table S4** Regression analysis for the production of FPase enzyme by *A. fumigatus* under SSF for quadratic response surface model fitting ANOVA. Where X1= pH, X2= Temperature and X3= Time.

Author contributions
NJ and KP; conceptualization. NJ and JG; methodology, formal analysis, writing—original draft. JG; writing—review and editing. LD; funding acquisition. KP; supervision. All authors reviewed the manuscript.

Availability of data and materials
All data generated or analyzed during this study are included in this article.

Declarations

Ethics approval and consent to participate
Not applicable.

Consent for publication
Not applicable.

Competing interests
The authors declare that they have no known competing financial interests or personal relationships that could have appeared to influence the work reported in this paper.

References

1. Nizami AS, Rehan M, Waqas M, Naqvi M, Ouda OKM, Shahzad K, et al. Waste biorefineries: enabling circular economies in developing countries. Bioresour Technol. 2017;241:1101–17.
2. Raina N, Slathia PS, Sharma P. Response surface methodology (RSM) for optimization of thermochemical pretreatment method and enzymatic hydrolysis of deodar sawdust (DS) for bioethanol production using separate hydrolysis and co-fermentation (SHCF). Biomass Convers Biorefinery. 2022;12:5175–95.
3. Cavali M, Soccol CR, Tavares D, Zevallos Torres LA, de Andrade O, Tanobe V, Zandoná Filho A, et al. Effect of sequential acid-alkaline treatment on physical and chemical characteristics of lignin and cellulose from pine (*Pinus* spp.) residual sawdust. Bioresour Technol. 2020;316:123884.
4. Liang C, Wang Q, Wang W, Lin CSK, Hu Y, Qi W. Enhancement of an efficient enzyme cocktail from *Penicillium* consortium on biodegradation of pretreated poplar. Chem Eng J. 2023;452:139352.
5. Fang L, Su Y, Wang P, Lai C, Huang C, Ling Z, et al. Co-production of xylo-oligosaccharides and glucose from birch sawdust by hot water pretreatment and enzymatic hydrolysis. Bioresour Technol. 2022;348:126795.
6. Amini N, Haritos VS, Tanksale A. Microwave assisted pretreatment of eucalyptus sawdust enhances enzymatic saccharification and maximizes fermentable sugar yield. Renew Energy. 2018;127:653–60.
7. Jin S, Zhang G, Zhang P, Fan S, Li F. High-pressure homogenization pretreatment of four different lignocellulosic biomass for enhancing enzymatic digestibility. Bioresour Technol. 2015;181:270–4.
8. Tavares D, Cavali M, de Tanobe OAV, Torres LAZ, Rozendo AS, Zandoná Filho A, et al. Lignin from residual sawdust of *Eucalyptus* spp.—Isolation, characterization, and evaluation of the antioxidant properties. Biomass. 2022;2:195–208.
9. Cavali M, Benbelkacem H, Kim B, Bayard R, Libardi Junior N, Gonzaga Domingos D, et al. Co-hydrothermal carbonization of pine residual sawdust and non-dewatered sewage sludge—effect of reaction conditions on hydrochar characteristics. J Environ Manage. 2023;340:117994.
10. Rominiyi OL, Adaramola BA, Ikumapayi OM, Oginni OT, Akinola SA. Potential utilization of sawdust in energy, manufacturing and agricultural industry; Waste to wealth. World J Eng Technol. 2017;05:526–39.
11. Olaiya BC, Lawan MM, Olonade KA. Utilization of sawdust composites in construction—a review. SN Appl Sci. 2023;5:140.
12. Mankar AR, Pandey A, Modak A, Pant KK. Pretreatment of lignocellulosic biomass: a review on recent advances. Bioresour Technol. 2021;334:125235.
13. Mondal S, Santra S, Rakshit S, Kumar Halder S, Hossain M, Chandra MK. Saccharification of lignocellulosic biomass using an enzymatic cocktail of fungal origin and successive production of butanol by *Clostridium acetobutylicum*. Bioresour Technol. 2022;343:126093.
14. Wu Y, Wen J, Su C, Jiang C, Zhang C, Wang Y, et al. Inhibitions of microbial fermentation by residual reductive lignin oil: Concerns on the bioconversion of reductive catalytic fractionated carbohydrate pulp. Chem Eng J. 2023;452:139267.
15. Uhrynowski W, Debiec K, Sklodowska A, Drewniak L. The role of dissimilatory arsenate reducing bacteria in the biogeochemical cycle of arsenic based on the physiological and functional analysis of *Aeromonas* sp. O23A. Sci Total Environ. 2017;598:680–9.
16. Drewniak L, Matlakowska R, Rewerski B, Sklodowska A. Arsenic release from gold mine rocks mediated by the activity of indigenous bacteria. Hydrometallurgy. 2010;104:437–42.
17. Matrawy AA, Marey HS, Embaby AM. The agro-industrial Byproduct Wheat Bran as an Inducer for Alkaline Protease (ALK-PR23) Production by Pschyrotolerant *Lysinibacillus sphaericus* Strain AA6 EMCCN3080. Waste Biomass Valoriz. 2023;11:1–6.
18. Azzouz Z, Bettache A, Djinni I, Boucherba N, Benallaoua S. Biotechnological production and statistical optimization of fungal xylanase by bioconversion of the lignocellulosic biomass residues in solid-state fermentation. Biomass Convers Biorefin. 2020;12:1–3.
19. Kumar M, Pandey AK, Kumari S, Wani SA, Jakeer S, Tiwari R, Prasad R, Gaur NA. Secretome produced by a newly isolated *Aspergillus flavus* strain in engineered medium shows synergy for biomass saccharification with a commercial cellulase. Biomass Convers Biorefin. 2020;11:1–3.
20. Liu D, Li J, Zhao S, Zhang R, Wang M, Miao Y, et al. Secretome diversity and quantitative analysis of cellulolytic *Aspergillus fumigatus* Z5 in the presence of different carbon sources. Biotechnol Biofuels. 2013;6:149.
21. Sharma Ghimire P, Ouyang H, Wang Q, Luo Y, Shi B, Yang J, et al. Insight into enzymatic degradation of corn, wheat, and soybean cell wall cellulose using quantitative secretome analysis of *Aspergillus fumigatus*. J Proteome Res. 2016;15:4387–402.
22. de Gouvêa PF, Bernardi AV, Gerolamo LE, de Souza SE, Riaño-Pachón DM, Uyemura SA, et al. Transcriptome and secretome analysis of *Aspergillus fumigatus* in the presence of sugarcane bagasse. BMC Genomics. 2018;19:232.
23. Adav SS, Ravindran A, Sze SK. Quantitative proteomic study of *Aspergillus Fumigatus* secretome revealed deamidation of secretory enzymes. J Proteomics. 2015;119:154–68.
24. Ziaei-Rad Z, Fooladi J, Pazouki M, Gummadi SN. Lignocellulosic biomass pre-treatment using low-cost ionic liquid for bioethanol production: an economically viable method for wheat straw fractionation. Biomass Bioenergy. 2021;151:106140.
25. Wang Z, Hou X, Sun J, Li M, Chen Z, Gao Z. Comparison of ultrasound-assisted ionic liquid and alkaline pretreatment of Eucalyptus for enhancing enzymatic saccharification. Bioresour Technol. 2018;254:145–50.
26. Lu X, Wang M, Zhao Z, Hu J, Zhang J, Liu P. Effect of different pretreatment of birch sawdust on the production of active polysaccharides by Inonotus obliquus under submerged fermentation and its structural mechanism. Appl Biochem Biotechnol. 2021;193:1545–57.
27. Joshi N, Grewal J, Matusik J, Drewniak L, Pranaw K. Faujasite Na-X zeolite as a novel carrier for cellulase immobilization and application in biomass saccharification. Biochem Eng J. 2023;198:109017.
28. Liu Z, Sun X, Hao M, Huang C, Xue Z, Mu T. Preparation and characterization of regenerated cellulose from ionic liquid using different methods. Carbohydr Polym. 2015;117:99–105.
29. Kruyeniski J, Ferreira PJT, da Videira Sousa Carvalho MG, Vallejos ME, Felissia FE, Area MC. Physical and chemical characteristics of pretreated slash pine sawdust influence its enzymatic hydrolysis. Ind Crops Prod. 2019;130:528–36.
30. Zabihi S, Sharafi A, Motamedi H, Esmaeilzadeh F, Doherty WOS. Environmentally friendly acetic acid/steam explosion/supercritical carbon dioxide system for the pre-treatment of wheat straw. Environ Sci Pollut Res Int. 2021;28:37867–81.
31. Ilanidis D, Stagge S, Jönsson LJ, Martín C. Hydrothermal pretreatment of wheat straw: effects of temperature and acidity on byproduct formation and inhibition of enzymatic hydrolysis and ethanolic fermentation. Agronomy. 2021;11:487.
32. Grewal J, Tiwari R, Khare SK. Secretome analysis and bioprospecting of lignocellulolytic fungal consortium for valorization of waste cottonseed cake by hydrolase production and simultaneous gossypol degradation. Waste Biomass Valorization. 2020;11:2533–48.
33. Sadaf A, Morya VK, Khare SK. Applicability of sporotrichum thermophile xylanase in the in situ saccharification of wheat straw pre-treated with ionic liquids. Process Biochem. 2016;51:2090–6.
34. Tiwari R, Singh S, Singh N, Adak A, Rana S, Sharma A, et al. Unwrapping the hydrolytic system of the phytopathogenic fungus *Phoma exigua* by secretome analysis. Process Biochem. 2014;49:1630–6.
35. Jin S, Zhang G, Zhang P, Li F, Fan S, Li J. Thermo-chemical pretreatment and enzymatic hydrolysis for enhancing saccharification of catalpa sawdust. Bioresour Technol. 2016;205:34–9.
36. Xu X, Lin M, Zang Q, Shi S. Solid state bioconversion of lignocellulosic residues by Inonotus obliquus for production of cellulolytic enzymes and saccharification. Bioresour Technol. 2018;247:88–95.
37. Tiwari R, Nain PKS, Singh S, Adak A, Saritha M, Rana S, et al. Cold active holocellulase cocktail from *Aspergillus niger* SH3: process optimization for production and biomass hydrolysis. J Taiwan Inst Chem Eng. 2015;56:57–66.
38. Tamura K, Stecher G, Kumar S. MEGA11: molecular evolutionary genetics analysis version 11. Mol Biol Evol. 2021;38:3022–7.
39. Sluiter A, Hames B, Ruiz R, Scarlata C, Sluiter J, Templeton D, et al. Determination of structural carbohydrates and lignin in biomass. Lab Anal Proced. 2008;1617:1–16.

40. Ghose TK. Measurement of cellulase activities. J Macromol Sci Part A Pure Appl Chem. 1987;59:257–68.
41. Wood TM, Bhat KM. Methods for measuring cellulase activities. Methods in Enzymology. Academic Press. 1988. 87–112.
42. Bradford M. A rapid and sensitive method for the quantitation of microgram quantities of protein utilizing the principle of protein-dye binding. Anal Biochem. 1976;72:248–54.
43. Wang Y, Wang Q, Huang H, Huang W, Chen Y, McGarvey PB, et al. A crowdsourcing open platform for literature curation in UniProt. PLoS Biol. 2021;19:e3001464.
44. Zhang H, Yohe T, Huang L, Entwistle S, Wu P, Yang Z, et al. dbCAN2: a meta server for automated carbohydrate-active enzyme annotation. Nucleic Acids Res. 2018;46:W95-101.
45. Segal L, Creely JJ, Martin AE, Conrad CM. An empirical method for estimating the degree of crystallinity of native cellulose using the X-Ray diffractometer. Text Res J. 1959;29:786–94.
46. Miller GL. Use of dinitrosalicylic acid reagent for determination of reducing sugar. Anal Chem. 1959;31:426–8.
47. Chen M, Zhao J, Xia L. Enzymatic hydrolysis of maize straw polysaccharides for the production of reducing sugars. Carbohydr Polym. 2008;71:411–5.
48. Singh A, Bajar S, Devi A, Bishnoi NR. Adding value to agro-industrial waste for cellulase and xylanase production via solid-state bioconversion. Biomass Convers Biorefin. 2023;13:7481–90.
49. Moran-Aguilar MG, Costa-Trigo I, Calderón-Santoyo M, Domínguez JM, Aguilar-Uscanga MG. Production of cellulases and xylanases in solid-state fermentation by different strains of *Aspergillus niger* using sugarcane bagasse and brewery spent grain. Biochem Eng J. 2021;172:108060.
50. Dias LM, dos Santos BV, Albuquerque CJB, Baeta BEL, Pasquini D, Baffi MA. Biomass sorghum as a novel substrate in solid-state fermentation for the production of hemicellulases and cellulases by *Aspergillus niger* and *A. fumigatus*. J Appl Microbiol. 2018;124:708–18.
51. Oliveira SD, de Araújo Padilha CE, Asevedo EA, Pimentel VC, de Araújo FR, de Macedo GR, et al. Utilization of agroindustrial residues for producing cellulases by *Aspergillus fumigatus* on Semi-Solid Fermentation. J Environ Chem Eng. 2018;6:937–44.
52. Hemansi GR, Kuhad RC, Saini JK. Cost effective production of complete cellulase system by newly isolated *Aspergillus niger* RCKH-3 for efficient enzymatic saccharification: medium engineering by overall evaluation criteria approach (OEC). Biochem Eng J. 2018;132:182–90.
53. Qi G, Huang D, Wang J, Shen Y, Gao X. Enhanced butanol production from ammonium sulfite pretreated wheat straw by separate hydrolysis and fermentation and simultaneous saccharification and fermentation. Sustain Energy Technol Assess. 2019;36:100549.
54. Kuila A, Rao PVC, Choudary NV, Gandham S, Velankar HR. Novel natural supplement for the production of fungal cellulases and application for enzymatic saccharification of wheat straw. Environ Prog Sustain Energy. 2015;34:1243–8.
55. Singhania RR, Saini JK, Saini R, Adsul M, Mathur A, Gupta R, et al. Bioethanol production from wheat straw via enzymatic route employing *Penicillium janthinellum* cellulases. Bioresour Technol. 2014;169:490–5.

Publisher's Note